ELSEVIER

Atherosclerosis 138 (1998) 281–288

ATHEROSCLEROSIS

Colocalization of iron and ceroid in human atherosclerotic lesions

Fan-Yen Lee [a], Tzong-Shyuan Lee [b], Ching-Chien Pan [b], An-Li Huang [c], Lee-Young Chau [b,*]

[a] *Department of Cardiovascular Surgery, Tri-Service General Hospital, Taipei, Taiwan, ROC*
[b] *Division of Cardiovascular Research, Institute of Biomedical Sciences, Academia Sinica, Nankang, Taipei, Taiwan, ROC*
[c] *Electron Microscopy Core Laboratory, Institute of Biomedical Sciences, Academia Sinica, Nankang, Taipei, Taiwan, ROC*

Received 8 September 1997; received in revised form 5 January 1998; accepted 22 January 1998

Abstract

The presence of ceroid, a complex of protein associated with oxidized lipids, is commonly observed in human atherosclerotic lesions. When the human aortic walls were examined by Perls' staining, it was found that the iron deposits were evident in aortas with atherosclerosis. The extent of iron deposition was associated with the severity of the lesion. Furthermore, the iron deposits appeared to be colocalized with ceroids either extracellularly or intracellularly in foam cell-like macrophages or smooth muscle cells. Electron microscopy and X-ray microanalysis revealed that some of the extracellular iron aggregates were present within the ceroids. Likewise, some of the subcellular iron aggregates were found to be located near the lipid droplets or within the ceroids of foam cells. Collectively, these observations support the theory that the lipid oxidation occurring in lipid-laden cells of aortic lesions is facilitated by iron-overload in these cells.

Keywords: Atherosclerosis; Iron; Ceroid

1. Introduction

Ceroid is an insoluble complex of oxidized lipid and protein found in all human atherosclerotic lesions [1–5]. Histologically, it is found within foam cells of the early lesions and appears as gruels or ring structures in the necrotic base of the advanced plaques [4,5]. It is generally believed to be, at least in part, resulted from the oxidation of low density lipoprotein (LDL) taken up by macrophages and/or smooth muscle cells in lesions [6–8]. The appearance of ceroid implicates the previous oxidative events occurring in local tissues. Since oxidation of lipid or LDL leads to the formation of a variety of products with diverse biological activities which have profound effects on the development of the plaques [9,10], it is of great importance to unravel the underlying mechanisms by which the oxidative process is initiated and propagated in vivo. In vitro studies have shown that small amounts of iron, which is the most important in vivo catalyst for oxidative free radical reactions, are required for oxidation of LDL by cultured endothelial cells [11], macrophages [12], and smooth muscle cells [13]. Furthermore, it has been shown that the interior of advanced human atherosclerotic lesions is a highly prooxidant environment, containing iron and copper ions, which are available to catalyze the free radical reactions as well as lipid peroxidation [14]. Recently, a study from our laboratory also demonstrated that iron deposition is prominent in human advanced atherosclerotic lesions [15]. Together, these observations have suggested the implication of iron in oxidative reactions in plaques. Nevertheless, direct evidence to support the association between iron and LDL/lipid oxidation is lacking. In the present study, we examined the distribution of ceroid and iron in specimens of human aortas. It was of great interest to find that the ceroid and iron colocalize either extracellularly or intracellularly in lipid-laden foam cells in advanced atherosclerotic lesions. This observation

* Corresponding author. Tel: +886 2 27899137; fax: +886 2 27829143; e-mail: lyc@ibms.sinica.edu.tw

0021-9150/98/$19.00
PII S0021-9150(98)00033-1

Table 1
Association between iron deposition and severity of atherosclerosis

Case	Sex/age	Aorta	Stage of lesion	Calcification	Iron deposition
01	M/75	Ascending	Normal	—	−
02	M/88	Abdominal	Advanced	+++	+++
03	M/72	Ascending	Normal	—	−
04	M/75	Ascending	Normal	—	−
05	M/53	Ascending	Normal	—	−
06	F/67	Ascending	Normal	—	−
07	F/68	Ascending	Normal	—	−
08	M/73	Abdominal	Advanced	++	+++
09	M/66	Ascending	Advanced	—	++
10	M/68	Ascending	Advanced	++	++
11	M/80	Ascending	Advanced	+++	+
12	M/16	Ascending	Normal	—	−
13	M/73	Abdominal	Advanced	+	+++
14	M/78	Abdominal	Advanced	++	++
15	M/42	Descending	Advanced	++	+++
16	M/16	Ascending	Early	—	+
17	M/70	Ascending	Advanced	+	+++
18	F/50	Ascending	Normal	—	−
19	M/40	Ascending	Early	—	−
20	M/43	Ascending	Advanced	—	++
21	M/45	Ascending	Normal	—	−
22	M/21	Ascending	Normal	—	−
23	F/67	Ascending	Normal	—	−
24	M/68	Ascending	Normal	—	−
25	M/75	Abdominal	Advanced	+++	+++
26	M/67	Abdominal	Advanced	+	+++

Calcification: —, not detectable; +, slight; ++, moderate; +++, severe.
Iron deposition: −, negative; +, positive stain with DAB amplification; ++, strong stain with DAB amplification; +++, blue stain with Perls' reaction without DAB amplification.

seems of some importance in supporting the notion that iron plays a detrimental role in atherosclerosis by promotion of lipid oxidation in lesions.

2. Materials and methods

2.1. Paraffin-embedded sections of human aortas

The human aortic specimens were obtained from patients during surgery for cardiovascular diseases. The collection of patient samples followed the procedure of the hospital ethical committee and the study was approved by the human subject review committee in our institute. Immediately after surgery, tissue samples were rinsed with ice-cold phosphate-buffered saline (PBS), fixed in 4% paraformaldehyde solution, and paraffin-embedded. Tissues were serially sectioned at 5-μm intervals and used for experiments thereafter.

2.2. Ceroid deposition

The ceroid deposits on lesions were examined by either lipid staining with 1% Sudan III for 1 h at room temperature or direct visualization under fluorescence microscope using a 580 nm filter.

2.3. Iron histochemistry

Iron deposition was examined by Perls' Prussian blue reaction [16]. In order to intensify the signal, after Perls' reaction, sections were incubated with 0.5% 3,3′-diaminobenzidine (DAB) in 0.1 M phosphate buffer pH 7.4 for 20 min, followed by 15 min in the same medium containing 0.01% H_2O_2. The reaction was stopped by rinsing in deionized H_2O for 30 min and then counterstained with hematoxylin or carmin red.

2.4. Immunohistochemistry

Paraffin sections were rehydrated and washed with PBS. Endogenous peroxidase activity was exhausted by incubation with 3% H_2O_2. Sections were then incubated with PBS containing 1% goat serum albumin and 1% bovine serum albumin for 30 min at 37°C. After three washes with PBS, sections were incubated with monoclonal antibody to human macrophage CD68 antigen (DAKO) (1:100) or to human smooth muscle cell α-actin (DAKO) (1:50) in PBS for 30 min at 37°C. After washing, sections were incubated with peroxidase-conjugated rabbit polyclonal antibody to mouse IgG (DAKO) (dilution 1:100) for another 30 min at 37°C.

Table 2
Distribution of iron and ceroid in human advanced atherosclerotic lesions

Sex/age	Aorta	Iron				Ceroid			
		Extracellular		Intracellular		Extracellular		Intracellular	
		Intima	Media	Mac.	SMC	Intima	Media	Mac.	SMC
M/88	Abdominal	+++	+++	+++	+++	++	+	+++	++
M/73	Abdominal	++	++	−	+++	++	+	−	++
M/80	Ascending	++	++	+	++	+	+	−	+
M/73	Abdominal	+++	+	+++	++	+++	+++	+++	+
M/78	Abdominal	++	++	+	++	+	+	++	++
M/43	Ascending	+	++	−	++	+	−	−	−
M/68	Ascending	++	++	−	++	−	−	−	−
M/75	Abdominal	+++	+++	−	+++	+++	+++	−	+++
M/67	Abdominal	+++	+++	+	+	++	++	+	++

Iron: −, negative; +, positive stain with DAB amplification; ++, strong stain with DAB amplification; +++, blue stain with Perls' reaction without DAB amplification.
Ceroid: −, negative; +, detectable by autofluorescence; ++, positive with Sudan III staining; +++, strong with Sudan III staining.

Color reactions were developed by incubation with glucose oxidase-DAB-nickel solution as described by Shu et al. [17]. After washing with tap water, sections were counterstained with carmine red. Negative control was performed by incubating sections with the secondary antibody alone.

2.5. Transmission electron microscopy

Tissues were fixed in 3% glutaraldehyde in 0.1 M Na-phosphate buffer overnight, washed with the same buffer for 15 min, and postfixed with 1% osmium tetroxide in 0.1 M phosphate buffer at room temperature for 2 h. Samples were dehydrated with a graded series of ethanol (50–100%) and then embedded in Spurr. The thin sections of 80 nm were prepared using ultramicrotome and placed on 200 or 300 mesh copper grids. Sections were stained with uranyl acetate and lead citrate and examined with a JEM 1200 EX transmission electron microscope at 80 kV. For subcellular localization of iron, tissues were fixed in 3% glutaraldehyde and incubated with fresh Perls' ferrocyanide solution at room temperature for 30 min prior to routine osmication and embedding [18].

2.6. X-Ray microanalysis

Thin sections from atherosclerotic lesions were carbonated and analyzed by X-ray microanalyzer attached to a JEM 1200 EX transmission electron microscope. This method was used to assess the iron content at sites of electron-dense precipitates within ceroids or near lipid droplets and at sites where precipitates were not evident by visual inspection. Acceleration voltage was 80 kV and acquisition times were 100 s. Three to four blocks were prepared from each atherosclerotic aorta. Three grids prepared from each block were randomly selected, examined and photographed. Two grids were selected from each block and 8–10 sites were assessed for iron content.

3. Results

A total of 26 human aortic samples were collected. Histological examination revealed that 12 of them were normal, two were early lesions with foam cells present in subendothelial intima and the rest were advanced fibrous lesions with necrotic cores and various degrees of calcification. The well-established Perls' Prussian blue method [16] was used to histochemically detect the iron-deposition in vessel walls. To increase the staining sensitivity, a modified procedure based on the ability of the Prussian blue ferric ferrocyanide complex to catalyze the oxidation of 3,3′-diaminobenzidine by hydrogen peroxide [19] was also used. As summarized in Table 1, Perls' staining demonstrated that iron deposition was not apparent in normal vessel walls or early lesions. However, the positive stains were commonly detected in advanced lesions, indicating its extent was closely associated with the severity of the lesions. Further experiments revealed that the iron deposits localize either extracellularly or intracellularly within cells of intima or media layers (Table 2). Furthermore, when the presence of ceroid was examined by either Sudan III lipid staining or autofluorescence, it was interesting to notice that the distribution of ceroid is similar to that of the iron deposition from the serial sections of same tissue block. As illustrated in Fig. 1, experiments performed on consecutive sections of an advanced lesion clearly demonstrated that the iron and ceroid colocalize extracellularly on the same region. Likewise,

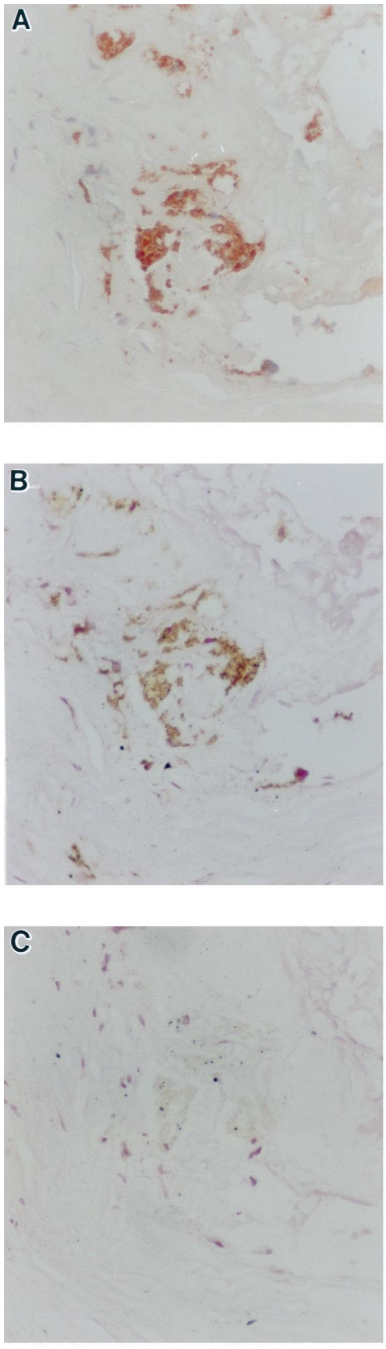

Fig. 1

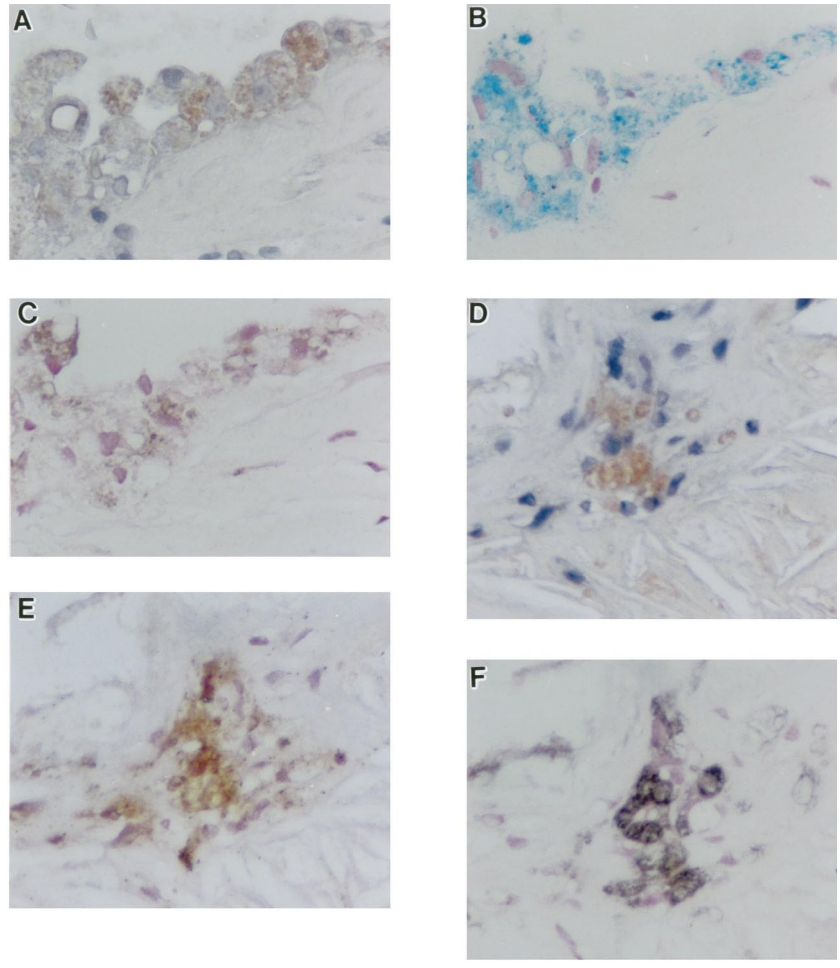

Fig. 2

Fig. 1. Extracellular colocalization of ceroid and iron in human atherosclerotic lesion. Sudan III dye staining (A) and Perls' reaction with DAB amplification (B) were conducted on consecutive sections from a human abdominal atherosclerotic aorta as described in Section 2. A control section (C) carried through the DAB intensification without preincubation with Perls' solution is a negative control for iron stain; A–C, magnification $\times 200$.

Fig. 2. Intracellular colocalization of ceroid and iron in foam-cell like macrophages. Serial sections (A–C and D–F) of human atherosclerotic aortas were subjected to Sudan III dye staining (A and D), iron staining (B and E), and immunostaining (C and F) with specific antibody against human macrophage CD68 antigen, respectively. Immunostaining conducted with secondary antibody alone was negative (data not shown). The blue stains in (B) indicate strong iron deposition detected by Perls' reaction without DAB amplification; A–C, magnification $\times 400$; D–F, $\times 400$.

the intracellular colocalization was also observed in foam cell-like macrophages which were identified by immunostaining with specific antibody to macrophage CD68 antigen (Fig. 2). Similar results were found in some lipid-laden smooth muscle cells which were immunostained with specific antibody to α-actin but not with specific antibody to macrophage CD68 antigen (Fig. 3). To further reveal the ultrastructural localiza-

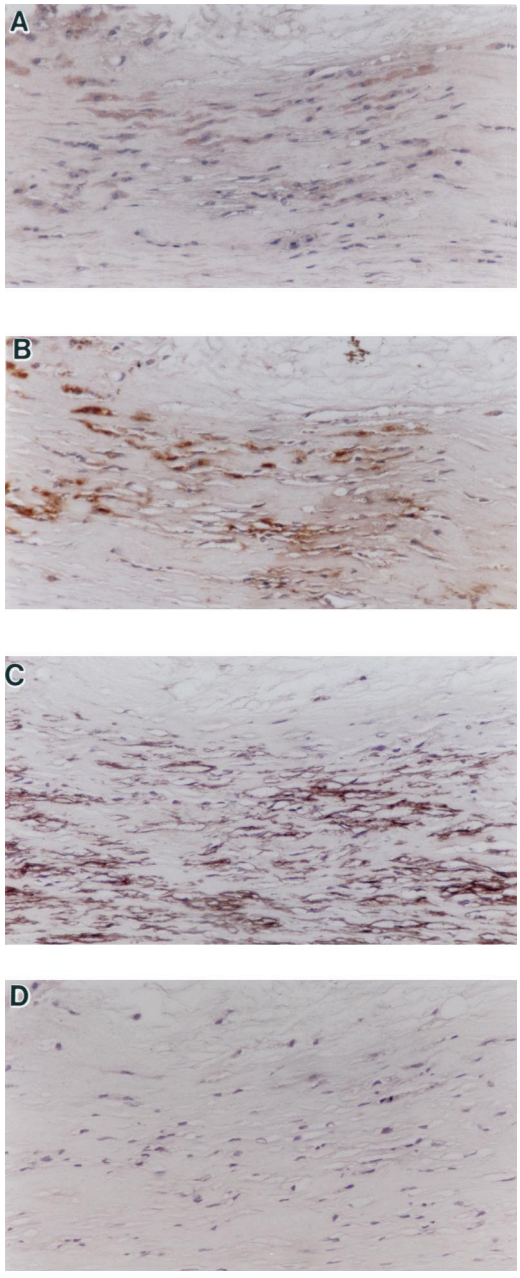

Fig. 3. Intracellular colocalization of ceroid and iron in foam-cell like smooth muscle cells. Lipid staining (A), iron staining (B), and immunostaining with specific antibody against smooth muscle cell α-actin (C) or macrophage CD68 antigen (D) were conducted on serial sections from a human atherosclerotic aorta as described in Section 2. Immunostaining conducted with secondary antibody alone was negative (data not shown); A–D, magnification × 200.

tion of iron and ceroids, the sections of advanced lesions were examined by transmission electron microscopy. As illustrated in Fig. 4, the extracellular ceroids were present as clusters of ring structures. When the specimens were treated with ferrocyanide solution prior to osmication and embedding, electron-dense precipitates were formed and visualized within these rings. To further confirm that these stain precipitates contained iron, sections were subjected to analysis by X-ray microbeam. As demonstrated in Fig. 4C, electron microbeam analysis of the sites containing the electron-dense precipitates revealed a small peak corresponding to iron. The iron peak was virtually not detectable in the nearby area without the precipitates (Fig. 4D). Experiments were also performed to examine the intracellular distributions of lipid and iron in foam cells. As shown in Fig. 5A, it was commonly observed that some of the iron aggregates, which were further confirmed by the X-ray microanalysis, locate proximately around the lipid droplets. Occasionally, the ultrastructural colocalization of ceroid ring structures and iron was also evident in these cells (Fig. 5B).

4. Discussion

Evidence is accumulating to show that oxidation of LDL in subendothelial intima is essential for the initiation of plaque formation in aortic walls [9,10]. However, the underlying mechanism(s) responsible for the oxidative reaction in vivo is not yet fully understood. The reactive oxygen species generated from enzymatic reactions of myeloperoxidase or lipoxygenase have been implicated in this process [20–24]. Nevertheless, the propagation of the peroxidation may be exacerbated by the reactions catalyzed by the transition-metals such as copper and iron [25]. Since previous studies from our laboratory and other investigators demonstrated the presence of iron in atherosclerotic lesions [14,15], we are interested in knowing whether iron is associated with the LDL/lipid oxidation and progression of the plaques in vivo. In the present study, we employed Perls' Prussian blue reaction, which is a well-established histological method for iron detection [16], to examine the localization of iron in vascular tissues. A modified procedure containing an additional DAB reaction [19] has been shown to increase the detection sensitivity and has been used successfully by other investigators [26,27]. Therefore, we also used the modified procedure for specimens showing weak or undetectable blue iron stains. Our results clearly demonstrated that the iron deposition in aortic walls is closely associated with the progression of atherosclerosis. Furthermore, it was found that ceroid and iron are colocalized in human advanced atherosclerotic lesions, suggesting that iron may play an important role in oxidative reactions during the development of atherosclerosis. The occurrence of iron and ceroid deposits, however, was not so evident in early lesions. It could be due to the limited sensitivity of the method employed in this study for the detection of iron and the lesser extent of the lipid oxidation which is not sufficient for the formation of the insoluble ceroids in the early lesions. Another possibility could be that iron deposition is not yet severe and

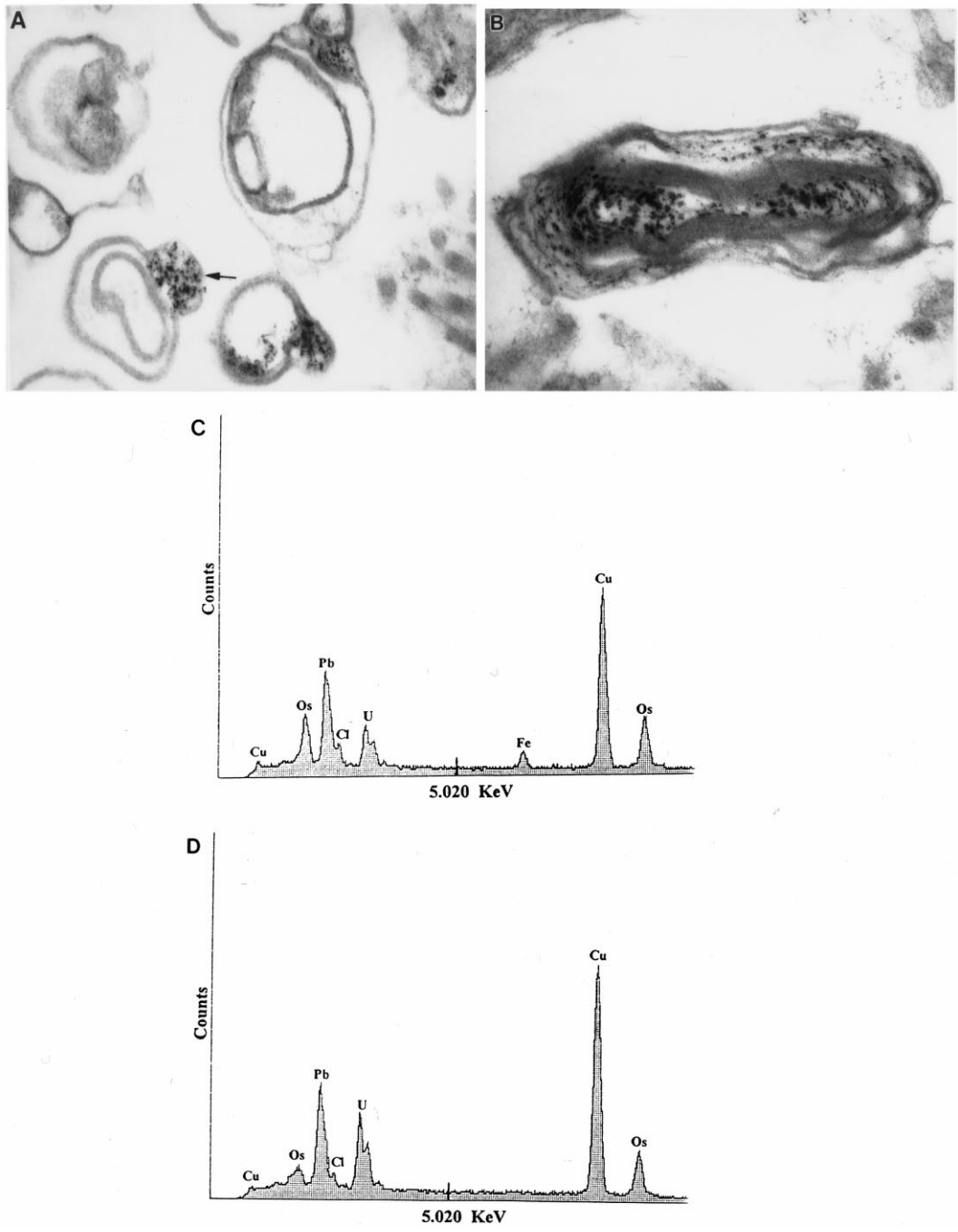

Fig. 4. Ultrastructural localization of extracellular ceroid and iron in human atherosclerotic lesions. The electron-dense precipitates were evident within the lipid ring structures (A and B). A, magnification $\times 50000$; B, $\times 75000$. The precipitates were not observed in sections without pretreatment with ferrocyanide solution (data not shown). C is the X-ray spectrum at sites of the electron-dense deposits as indicated by the arrow. D is the spectrum obtained at sites where deposits were not apparent.

it may have little effect on the initiation of the lipid oxidation in the early stage. Nevertheless, in vitro studies on macrophage [28] or cardiac myocyte [29] cultures have demonstrated that iron could promote the oxidation of LDL or lipid and the accumulation of ceroids in these cells. Therefore, the potential role of iron involved in the oxidation of lipids in the early stages of plaque formation awaits to be further elucidated.

It was of great interest to observe the colocalization of ceroid and iron in foam cells. Although macrophages are believed to be the primary cell type to become foam cells in atherosclerotic lesions, previous reports from other laboratories demonstrated the presence of smooth muscle cell-derived foam cells in atherosclerotic plaques of humans and experimental animals [30–33]. In the present study, we also identified some of the lipid-laden

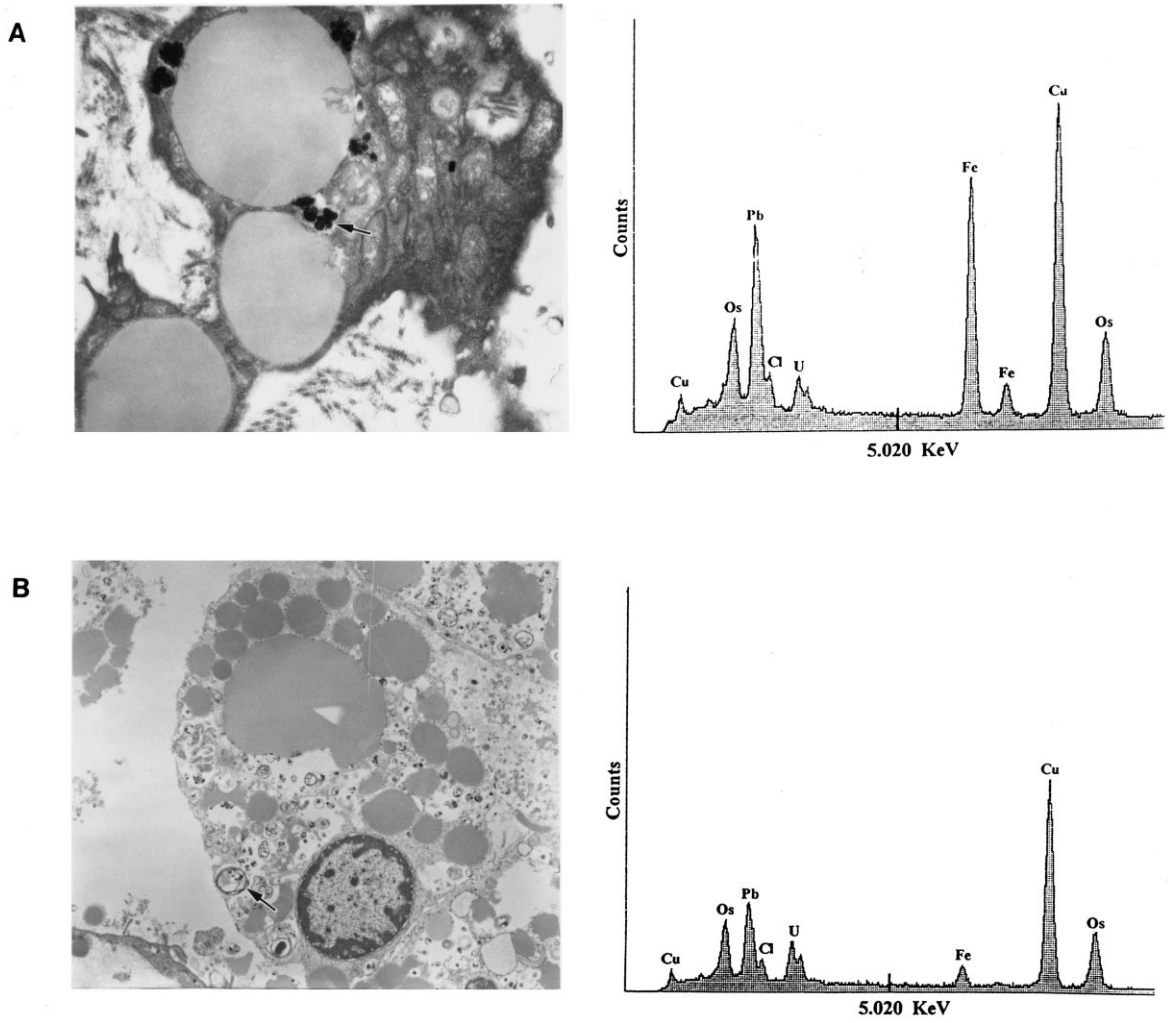

Fig. 5. Ultrastructural localization of intracellular lipid and iron in foam cells of human atherosclerotic lesions. The electron-dense iron aggregates locate closed to the lipid droplets (A) or membranous ceroids (B) in foam cells. A, magnification $\times 12000$; B, $\times 4000$. The X-ray spectra were obtained from the sites of electron-dense deposits as indicated by arrows.

cells to be of smooth muscle cell-origin, as revealed by the positive immunostaining with specific antibody to α-actin but not with specific antibody to macrophage CD68 antigen. The localization of both ceroids and iron at ultrastructural levels was further examined by transmission electron microscopy and X-ray microanalysis. Similar to those previously reported by others [4,5], the extracellular insoluble ceroids appear as membranous ring structures. Furthermore, it was intriguing to see that the electron-dense iron aggregates were associated with these rings. The subcellular ceroids/lipid droplets and iron were also found to be ultrastructurally colocalized within the lipid-laden cells. Taken together, these observations apparently strongly support the close association between iron and ceroid formation in atherosclerotic lesions.

In conclusion, the histological examination of human aortic tissues clearly demonstrates that iron and ceroid deposits are colocalized in atherosclerotic lesions, suggesting that iron may play an important role in exacerbating the oxidation of LDL/lipids and accelerating the progression of atherosclerosis. The origin of iron deposited in plaques is an intriguing issue remaining to be resolved.

Acknowledgements

This work is supported by a grant for the Clinical Research Centers from the Institute of Biomedical Sciences, Academia Sinica, Taiwan.

References

[1] Pappenheimer AM, Victor J. 'Ceroid' pigment in human tissues. Am J Pathol 1946;22:395.

[2] Burt RC. The incidence of acid-fast pigment (ceroid) in aortic atherosclerosis. Am J Clin Pathol 1952;22:135.
[3] Mitchinson MJ. Insoluble lipids in human atherosclerotic plaques. Atherosclerosis 1982;45:11.
[4] Mitchinson MJ, Hothersall DC, Brooks PN, De Burbure CY. The distribution of ceroid in human atherosclerosis. J Pathol 1985;145:177.
[5] Ball RY, Carpenter KLH, Mitchinson MJ. What is the significance of ceroid in human atherosclerosis? Arch Pathol Lab Med 1987;111:1134.
[6] Ball RY, Bindman JP, Carpenter KLH, Mitchinson MJ. Oxidized low density lipoprotein induces ceroid accumulation by murine peritoneal macrophages in vitro. Atherosclerosis 1986;60:173.
[7] Shimasaki H, Maeba R, Tachibana R, Ueta N. Lipid peroxidation and ceroid accumulation in macrophages cultured with oxidized low density lipoprotein. Gerontology 1995;41(Suppl 2):39.
[8] Hoff HF, Hoppe G. Structure of cholesterol containing particles accumulating in atherosclerotic lesions and the mechanisms of their derivation. Curr Opin Lipidol 1995;6:317.
[9] Ross R. The pathogenesis of atherosclerosis: a perspective for the 1990s. Nature 1993;362:801.
[10] Berliner JA, Navab M, Fogelman AM, Frank JS, Demer LL, Edwards PA, Watson AD, Lusis AJ. Atherosclerosis: basic mechanisms, oxidation, inflammation, and genetics. Circulation 1995;91:2488.
[11] Morel DW, DiCorleto PE, Chisolm GM. Endothelial and smooth muscle cells alter low density lipoprotein in vitro by free radical oxidation. Atherosclerosis 1984;4:357.
[12] Henriksen T, Mahoney EM, Steinberg D. Enhanced macrophage degradation of biologically modified low density lipoprotein. Arteriosclerosis 1983;3:149.
[13] Heinecke JW, Baker L, Rosen H, Chait A. Superoxide-mediated modification of low density lipoprotein by arterial smooth muscle cells. J Clin Invest 1986;77:757.
[14] Smith C, Mitchinson MJ, Aruoma OI, Halliwell B. Stimulation of lipid peroxidation and hydroxyl-radical generation by contents of human atherosclerotic lesions. Biochem J 1992;286:901.
[15] Pang J-HS, Jiang M-J, Chen Y-L, Wang F-W, Wang DL, Chu S-H, Chau L-Y. Increased ferritin gene expression in atherosclerotic lesions. J Clin Invest 1996;97:2204.
[16] Perls M. Nachweis von Eisenoxyd in gewissen Pigmenten. Virchows Arch Pathol Anat 1967;39:42.
[17] Shu S, Ju G, Fan L. The glucose oxidase-DAB-nickel method in peroxidase histochemistry of the nervous system. Neurosci Lett 1988;85:169.
[18] Parmley RT, Spicer SS, Alvarez CJ. Ultrastructural localization of nonheme cellular iron with ferrocyanide. J Histochem Cytochem 1978;26:729.
[19] Nguyen-Legros J, Bizot J, Bolesse M, Pulicani J-P. Noir de Diaminobenzidine: Une nouvelle methode histochimique de revelation du fer exogene. Histochemistry 1980;66:239.
[20] Daugherty A, Dunn JL, Rateri DL, Heinecke JW. Myeloperoxidase, a catalyst for lipoprotein oxidation, is expressed in human atherosclerotic lesions. J Clin Invest 1994;94:437.
[21] Ylä-Herttuala S, Rosenfeld ME, Parthasarathy S, Sigal E, Sarkioja T, Witzum JL, Steinberg D. Gene expression in macrophage-rich human atherosclerotic lesions. 15-Lipoxygenase and acetyl low density lipoprotein receptor messenger RNA colocalize with oxidation specific lipid-protein adducts. J Clin Invest 1991;87:1146.
[22] Folcik VA, Nivar-Aristy RA, Krajewski LP, Cathcart MK. Lipoxygenase contributes to the oxidation of lipids in human atherosclerotic plaques. J Clin Invest 1995;96:504.
[23] Hazen SL, Heinecke JW. 3-Chlorotyrosine, a specific marker of myeloperoxidase-catalyzed oxidation, is markedly elevated in low density lipoprotein isolated from human atherosclerotic intima. J Clin Invest 1997;99:2075.
[24] Kühn H, Heydeck D, Hugou I, Gniwotta C. In vivo action of 15-lipoxygenase in early stages of human atherogenesis. J Clin Invest 1997;99:888.
[25] Rice-Evans C, Burdon R. Free radical–lipid interactions and their pathological consequences. Prog Lipid Res 1993;32:71.
[26] Hill JM, Switzer RC. The regional distribution and cellular localization of iron in the rat brain. Neuroscience 1984;11:595.
[27] Kondo Y, Ogawa N, Asanuma M, Ota Z, Mori A. Regional differences in late-onset iron deposition, ferritin, transferrin, astrocyte proliferation, and microglial activation after transient forebrain ischemia in rat brain. J Cereb Blood Flow Metab 1995;15:216.
[28] Yuan X-M, Brunk UT, Olsson AG. Effects of iron- and hemaglobin-loaded human monocyte-derived macrophages on oxidation and uptake of LDL. Arterioscler Thromb Vasc Biol 1995;15:1345.
[29] Marzabadi MR, Sohal RS, Brunk UT. Effect of ferric iron and desferrioxamine on lipofuscin accumulation in cultured rat heart myocytes. Mech Aging Dev 1988;46:145.
[30] de la Llera Moya M, Rothblat GH, Glick JM, England JM. Etoposide treatment suppresses atherosclerotic plaque development in cholesterol-fed rabbits. Arterioscler Thromb 1992;12:1363.
[31] Ikeda T, Shirasawa T, Esaki Y, Yoshiki S, Hirokawa K. Osteopontin mRNA is expressed by smooth muscle-derived foam cells in human atherosclerotic lesions of the aorta. J Clin Invest 1993;92:2814.
[32] Spagnoli LG, Orlandi A, Marino B, Mauriello A, De-Angelis C, Ramacci MT. Propionyl-L-carnitine prevents the progression of atherosclerotic lesions in aged hyperlipemic rabbits. Atherosclerosis 1995;114:29.
[33] Li H, Freeman MW, Lippy P. Regulation of smooth muscle cell scavenger receptor expression in vivo by atherogenic diets and in vitro by cytokine. J Clin Invest 1995;95:122.